

Wave associated anomalous drag during magnetic field reconnection

F. S. Mozer,¹ M. Wilber,¹ and J. F. Drake²

¹Space Sciences Laboratory, University of California, Berkeley, California 94720, USA

²University of Maryland, College Park, Maryland 20742, USA

(Received 26 July 2011; accepted 8 September 2011; published online 14 October 2011)

The anomalous drag, \mathbf{D} , due to large amplitude plasma waves is used for the first time, in place of $\eta^*\mathbf{j}$, to estimate dissipation at the sub-solar magnetopause and to determine the extent to which this drag accounts for the reconnection electric field. This anomalous drag is determined by measuring correlations of the fluctuations in the electric field and plasma density. Large amplitude electric fields occurred more than 60% of the time in the more than 100 sub-solar, low latitude magnetopause crossings of the THEMIS satellite. They occurred mainly near the magnetospheric separatrix in the form of electrostatic lower hybrid and whistler waves. The anomalous drag at the separatrix was generally $<10\%$ of the average reconnection electric field, and it was $<1\%$ of the field in the current sheet. Thus, anomalous drag due to waves is not a significant driver of reconnection or of the required dissipation at the sub-solar magnetopause. © 2011 American Institute of Physics. [doi:10.1063/1.3647508]

I. INTRODUCTION

Large amplitude plasma waves are observed in many regions of space, including the terrestrial magnetosphere, the magnetopause, magnetosheath, bow shock, and solar wind. Dissipation due to these waves has been estimated by adding the *ad-hoc* term, $\eta^*\mathbf{j}$, to the electron fluid equation of motion or to the Generalized Ohm's Law,¹ where η^* is the anomalous resistivity and \mathbf{j} is the plasma current density. The rationale for this term comes from electric circuits where the electric field in a resistor is proportional to the current through it. This proportionality does not arise from a fundamental principle. Rather it results from observations in materials that are called ohmic because they obey Ohm's Law. Many materials, including plasmas,² are not ohmic materials. Thus, anomalous resistivity in plasmas must be replaced by terms resulting from a rigorous derivation.³ A brief description of these terms follows.

Newton's Second Law for an element of electron fluid in a collisionless plasma is

$$n\mathbf{E} = -nm(\partial\mathbf{U}_e/\partial t + \mathbf{U}_e \cdot \nabla\mathbf{U}_e) - n\mathbf{U}_e \times \mathbf{B} - \nabla \cdot \mathbf{P}_e, \quad (1)$$

where n = plasma density, \mathbf{U}_e = electron bulk velocity, \mathbf{P}_e = electron pressure tensor, and m = electron mass.

Defining the fluctuating Y-component of the electric field as $\delta E_Y = [E_Y - \langle E_Y \rangle]$ and the fluctuating plasma density as $\delta n = [n - \langle n \rangle]$, the left side of Eq. (1) becomes $[e\langle n \rangle \langle E_Y \rangle + e\delta n \delta E_Y + e\langle E_Y \rangle \delta n + e\langle n \rangle \delta E_Y]$. After averaging this expression and Eq. (1) over many oscillations of the fluctuating components, one obtains³

$$\langle E_Y \rangle = -\langle nm(\partial\mathbf{U}_e/\partial t + \mathbf{U}_e \cdot \nabla\mathbf{U}_e)_Y \rangle / e\langle n \rangle - \langle n\mathbf{U}_e \times \mathbf{B} \rangle_Y / \langle n \rangle - \langle \nabla \cdot \mathbf{P}_e \rangle_Y / e\langle n \rangle + D_Y, \quad (2)$$

where

$$D_Y = \text{Anomalous drag due to waves} \equiv -\langle \delta n \delta E_Y \rangle / \langle n \rangle. \quad (3)$$

The averaging of Eq. (2) is spatial while the only averaging of single satellite data has to be temporal. Because the spacecraft moves relative to the magnetopause, it is assumed that these two averages are the same. A viscous transport term due to waves is also derived in a similar way.³ It is not discussed here because all of its terms have not been measured in any space experiment.

D_Y of Eq. (2) provides dissipation required for converting electromagnetic energy to plasma energy and it also contributes to the reconnection electric field, E_Y that is required for reconnection to occur. Thus, the measurement of D_Y , described below for the first time, is fundamental to the understanding of magnetic field reconnection.

II. DATA

Figure 1 is a plot of wave amplitudes observed at a typical sub-solar magnetopause crossing. This and the data in later figures is plotted in minimum variance coordinates with X normal to the current sheet and pointing generally sunward, Z in the direction of the reconnecting magnetic field and pointing generally perpendicular to the ecliptic plane, and Y, the third component, points generally eastward. During the seven second interval of the plot, the spacecraft passed from the magnetosphere, through the current sheet, and into the magnetosheath. Associated with this crossing, the plasma density of panel b increased by an order-of-magnitude and the reconnection magnetic field of panel f changed from the magnetospheric value of +60 nT to the magnetosheath value of -20 nT. This case exhibits a strong asymmetry, with the ratio of $|B_Z|/n$ differing by a factor of 30 across the current layer. The Hall term in the Generalized Ohm's law is proportional to $|B_Z|/n$, so it varies greatly across the magnetopause. All other events in the present study exhibit similar asymmetries which result in wave and other properties that differ significantly from those of the

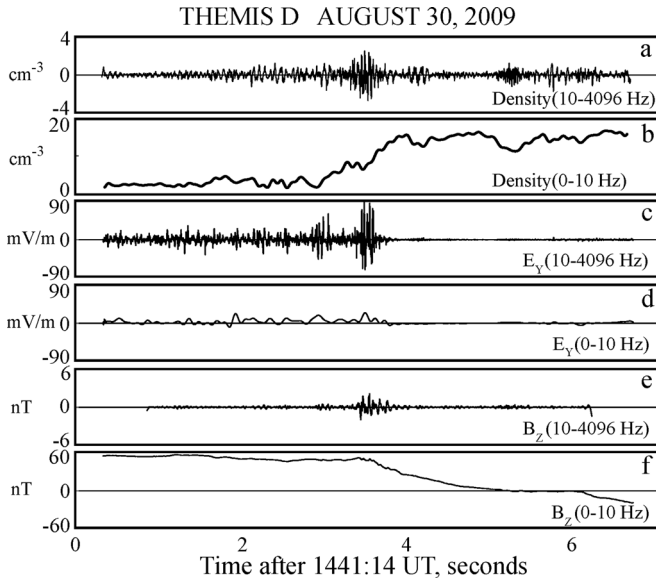


FIG. 1. Typical example of wave amplitudes at a sub-solar magnetopause crossing.

more-often studied but less-often observed (except in the magnetotail) symmetric reconnection.

By pairs, the successive panels in Fig. 1 present high frequency and 0–10 Hz components of the plasma density, E_Y , and B_Z . The largest amplitude waves occur near a time of 3.5 s at the magnetospheric separatrix, which is the magnetospheric boundary of the out-of-plane current sheet determined from the changing field in panel f. The plasma density in panel b at this time was about 10 cm^{-3} , while the amplitude of the density fluctuations in panel a was about 1 cm^{-3} . Thus, $\langle |\delta n| \rangle / \langle n \rangle$ was about 0.1. From panels c and d, one may estimate that $\langle |\delta E_Y| \rangle / \langle E_Y \rangle$ was about 5. Thus,

$$[\langle |\delta n| \rangle \langle |\delta E_Y| \rangle / \langle n \rangle] \sim 0.5 \langle E_Y \rangle \quad (4)$$

at the magnetospheric separatrix, which suggests that the anomalous drag of Eq. (3) would be important at this location if the correlation between δn and δE_Y (which is not included in Eq. (4)) is large. It is one purpose of the present paper to compute such correlations in the estimate of the anomalous drag not only at the separatrix but also through the current sheet where the fluctuations are orders-of-magnitude smaller.

In a similar manner, from panels e and f of Fig. 1, an estimate of $\langle |\delta B_Z| \rangle / \langle B_Z \rangle$ is ~ 0.02 at the separatrix and much less in the current sheet. This suggests that, for the fluctuating component of $ne\mathbf{U}_e \times \mathbf{B}$ in Eq. (2) to be important, the fluctuations of \mathbf{U}_e must be larger than 50 times the average value of \mathbf{U}_e . These fluctuations have never been measured. However, such a large value of the fluctuating electron flow is highly unlikely, which means that it is highly unlikely that electromagnetic waves contribute significantly to the anomalous drag anywhere at the magnetopause.

During the fall of 2010, more than 100 crossings of the sub-solar magnetopause near the equatorial plane by the THEMIS D spacecraft were examined to find that more than 60% of the crossings had large amplitude electric field waves, where a large amplitude wave is one whose amplitude is

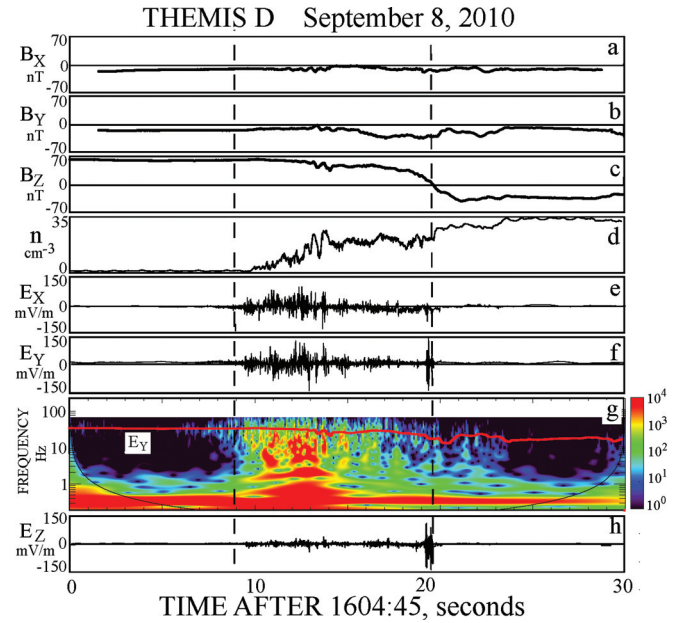


FIG. 2. (Color) The plasma density, electric field and magnetic field during a satellite crossing of the sub-solar magnetopause. The red line in panel (g) gives the lower hybrid frequency while the cone of influence (the black line) delineates the frequency below which the data are uncertain because the transform method necessarily includes significant edge effects. The color scale gives power in arbitrary units.

greater than that of the three-second-spin-period averaged field. The typical duration of the wave field in these events was about 10% of the magnetopause crossing time with the longest events lasting up to 50% of the crossing. Ninety percent of the large amplitude wave events occurred near the magnetospheric separatrix, 10% were in the current layer and 6% were in the magnetosheath (the sum is greater than 100 because of events that occurred in both the current layer and the magnetospheric separatrix). The wave amplitude was greatest at the magnetospheric separatrix. The two predominant frequency bands observed were below the lower hybrid frequency and between the lower hybrid frequency and half of the electron gyrofrequency, with roughly comparable occurrence frequencies. The spacecraft potential served as a proxy for the plasma density⁴ that was needed to compute D . To perform this analysis, the experimental data have been averaged over time (0.25 s) as the spacecraft crossed the current sheet.

An asymmetric magnetopause crossing having large amplitude waves only near the magnetospheric separatrix is illustrated in Fig. 2, at a time when the THEMIS spacecraft was at 9.9 Earth radii from the center of the earth, at a magnetic local time of 13:48, and a magnetic latitude of less than 3° . Descriptions of THEMIS instruments, measurements and some earlier electric field analyses are given elsewhere.^{5,6} Panel (c) of Fig. 2 shows that the reconnecting component of the magnetic field varied from about 65 nT in the magnetosphere near the beginning of the plot, to about -35 nT in the magnetosheath near the end of the plot. Associated with this change across the current layer, the plasma density of panel (d) increased from about 0.7 to 35 cm^{-3} . The guide field for this crossing (given by the ratio of the average B_Y in the asymptotic regions to the average $|B_Z|$ in the two regions) was about 0.25, and the electron beta for this entire event was less than one.

Panels (e), (f), and (h) of Fig. 2 give the three components of the electric field in a minimum variance of B coordinate system. The wave electric field was as great as 200 mV/m. During the large amplitude wave, the average angle between the fluctuating electric field and the background magnetic field was $89.5^\circ \pm 1.7^\circ$. The event occurred mainly on the magnetospheric side of the current layer near the magnetospheric separatrix and its duration was about a third of the total crossing time. There was little electric field power in the main current layer or in the magnetosheath. The electric field and plasma density data between the two vertical dashed lines in Fig. 2 were obtained at 8192 samples/second while the remaining data were obtained at 128 samples/s. Thus, the lower hybrid frequency range (25–50 Hz) was well covered while higher frequency modes were only examined in the central region of the plot and found to be negligible.

Panel (g) of Fig. 2 is a wavelet spectrogram⁷ of E_Y obtained from the data at 128 samples/second. The red curve in this panel is the lower hybrid frequency, and it is noted that the main wave was both below the lower hybrid frequency and confined to the region around the magnetospheric separatrix. (The line at ~ 0.3 Hz is noise at the spin frequency.) Although the measurement capability extended to 4 kHz in the turbulent region, the power in the fluctuating signals fell rapidly above the lower hybrid frequency.

Figure 3 presents the 0.25 s averages of the reconnecting magnetic field, B_Z , the out-of-plane electric field, E_Y , and the drag, D_Y , of Eq. (3), computed over the lower hybrid frequency range of 4–50 Hz. Also shown, as the dashed line, is $0.1v_A B_Z$, the out-of-plane electric field expected from earlier simulations and data, where v_A is the average Alfvén speed in the asymptotic regions. While there is a correlation between the electric field and D_Y near the magnetospheric separatrix (where the wave amplitude was largest), D_Y accounts for no more than about 10% of the observed electric field in this region. More importantly, through the current layer, the mag-

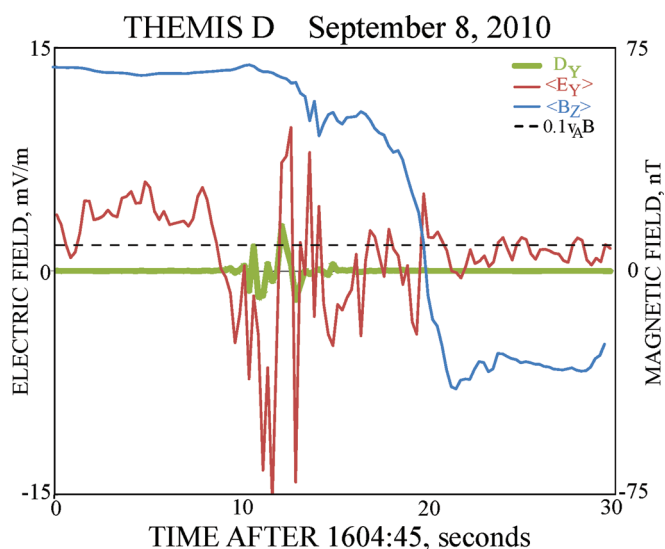


FIG. 3. (Color) Quarter second averages of the magnetic field, the out-of-plane electric field, and the anomalous drag, D_Y . Note that the anomalous drag was absent in the current layer and elsewhere other than near the magnetospheric separatrix, where it accounted for $\sim 10\%$ of the observed electric field.

nitude of D_Y was not greater than 1% of the average E_Y . Frequencies outside of the band of 4–50 Hz made an even smaller contribution to D_Y . Thus, for this event, lower hybrid drag is present but unimportant for dissipation and for supporting the out-of-plane electric field at the magnetospheric separatrix and it is irrelevant in the current layer.

Six magnetopause crossings with lower hybrid turbulence have been analyzed in detail. For many of these crossings, D_X , D_Z , and D_{\parallel} were also measured with results similar to those described above. Although one must be careful about drawing general conclusions from this amount of data, the following points may be made:

1. Wave power was not observed inside the current layer or in the magnetosheath during these six crossings.
2. The turbulence and anomalous drag were associated with the lower hybrid drift instability because:
 - The spectra were peaked at and below the lower hybrid frequency.
 - The wave electric field was nearly perpendicular to the background magnetic field.
 - The largest waves were located at density gradients.
3. The observed lower hybrid waves were electrostatic because:
 - The correlations of δE_Y with δB_Z or δB_X were weak. The correlation coefficients fluctuated randomly over the range of -0.3 to $+0.3$.
 - In regions of large electric fields and anomalous drag, the measured $\delta E_Y/\delta B_Z$ and $\delta E_Y/\delta B_X$ were $\geq 0.1c$, which is at least an order-of-magnitude larger than ω/k obtained from the dispersion relation for electromagnetic lower hybrid waves in a warm, magnetized plasma,¹⁰ for waves whose wavelengths were less than 30 ion skin depths (3500 km).

Electrostatic lower hybrid waves interact resonantly with both electrons and ions. This allows them to mediate the transfer of energy and momentum between the two species and to cause energy conversion and plasma heating via Eq. (3). That these processes were generally observed near the magnetospheric separatrix but not in the current layer is consistent with simulations that showed the instability at the edge of the current sheet.^{11,12} Other work has suggested that electromagnetic lower hybrid waves exist in the current layer itself.¹³ A laboratory experiment measured such waves and suggested that they enhance the reconnection rate.¹⁴ Such waves have not yet been observed in the space data, which were in a different plasma parameter regime.

Figure 4 provides an example of magnetopause waves at frequencies above the lower hybrid frequency. It was obtained at 9.3 Earth radii, a local time of 09:30 and a latitude of 4° . Panel (c) of this figure shows that the reconnecting magnetic field varied from -25 nT in the magnetosheath, at the beginning of the six second crossing, to 55 nT in the magnetosphere at the end of the plot. The plasma density of panel (d) did not vary greatly during this crossing although it did decrease at a later time. The 80 mV/m waves in the electric field panels (e), (f), and (h) occurred near the magnetospheric separatrix (as seen from the slope of B_Z in panel (c)) and they lasted for about 0.3 s or 5% of the crossing time.

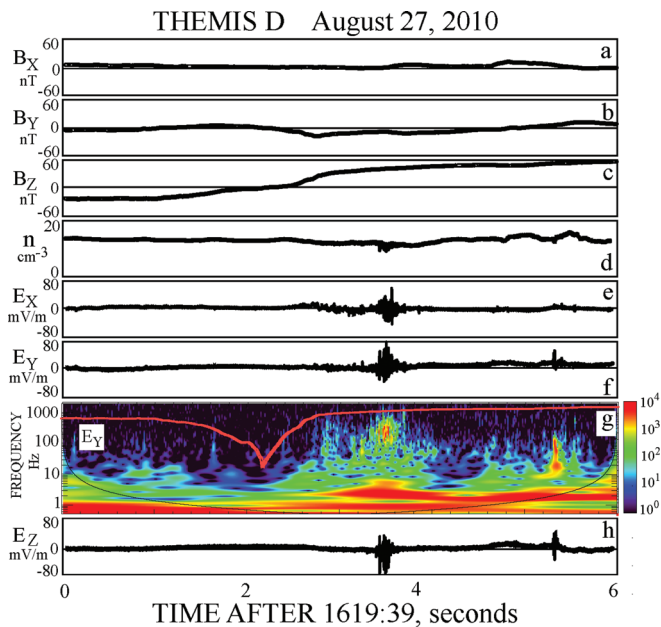


FIG. 4. (Color) The plasma density, electric field, and magnetic field during a satellite crossing of the dayside magnetopause. The red line in panel (g) gives the electron gyrofrequency while the cone of influence (the black line) delineates the frequency below which the data are uncertain because the transform method necessarily includes significant edge effects. The color scale gives power in arbitrary units.

The wavelet spectrogram in panel (g) of Fig. 4 shows that the turbulent power was above the lower hybrid frequency and below about half of the electron gyrofrequency (given by the red curve). That there was little power observed in the current layer or magnetosheath is consistent with a previous conclusion that the vicinity of the X-line is not the most interesting location for field measurements.^{8,9} The magnetic field decreased to less than 1 nT in the current sheet and this caused the electron gyrofrequency to dip to about 18 Hz. The guide magnetic field for this event was less than 0.1 and the electron beta was less than one everywhere except during the 1 s interval surrounding the minimum in the electron gyrofrequency. It is also noted that the wave power at frequencies above half of the electron gyrofrequency was small.

D_Y correlated with $\langle E_Y \rangle$ in the large field region but its magnitude was less than 1% of $\langle E_Y \rangle$ (not shown). During the 2 s crossing through the main current layer, the magnitude of D_Y was less than $10^{-4} \langle E_Y \rangle$. Thus, for this crossing also, anomalous drag was unimportant for dissipating electromagnetic energy or for supporting the reconnection electric field in the current layer.

The observed waves were electrostatic whistler mode waves because:

- They were in the frequency range above the lower hybrid frequency and below half of the electron gyrofrequency.
- The ratio, E/B , was greater than 3c.
- The observed gradient in the electron temperature may have provided the free energy for the instability.
- The wave spectrum is similar to that reported in a laboratory experiment on electrostatic whistler mode waves.¹⁵

It is noted that lower hybrid waves were not observed during the crossing of Fig. 4, perhaps because there was no density gradient to support the lower hybrid instability.

III. DISCUSSION

Electrostatic whistler and lower hybrid waves have been observed in sub-solar, equatorial magnetopause crossings. They occur mainly at the magnetospheric separatrix and they are largely absent in the current layer or in the magnetosheath. The anomalous drag, D_Y , computed from correlations of the fluctuations in E_Y and the plasma density, is less than 10% of the average E_Y at the magnetospheric separatrix and D_Y is even smaller through the reconnection current layer. Thus, anomalous drag cannot account for the dissipation associated with reconnection nor is it sufficient to explain a major portion of the electric field required for magnetic field reconnection to occur.

Possible explanations for the absence of significant wave activity in the current layers studied in this investigation are that wave processes are not important there⁸ or that the space observations were made far from the X-line where such processes may not be important even though simulations show that significant dissipation occurs far from the X-line.⁸ While it is not generally known at what distance from the X-line most crossings occurred, one or more crossings through the X-line to within a few electron skin depths have been found by detailed examination of the particle distributions. These crossings show that the fields and waves at this location are also insufficient for providing the required drag. These crossings are the subject of a further publication.

ACKNOWLEDGMENTS

This work was supported by NASA Grant Nos. NNX09AE41G-1/11, NNX09AI02G, and NASA Contract No. NAS5-02099-07/10. We also thank Dr. Chris Chaston for many helpful discussions.

- ¹I. Silin, J. Buchner, and A. Vaivads, *Phys. Plasmas* **12**, 062902 (2005) and references therein.
- ²J. F. Drake, M. Swisdak, C. Cattell, M. A. Shay, B. N. Rogers, and A. Zeiler, *Science* **299**, 7 (2003).
- ³H. Che, J. F. Drake, and M. Swisdak, *Nature (London)* **474**, 184 (2011).
- ⁴J. D. Scudder, X. Cao, and F. S. Mozer, *J. Geophys. Res.* **105**, A9, doi:10.1029/1999JA900423 (2000).
- ⁵V. Angelopoulos, D. Sibeck, C. W. Carlson, J. P. McFadden, D. Larson, R. P. Lin, J. W. Bonnell, F. S. Mozer, R. Ergun, C. Cully, K. H. Glassmeier, U. Auster, A. Roux, O. LeContel, S. Frey, T. Phan, S. Mende, H. Frey, E. Donovan, C. T. Russell, R. Strangeway, J. Liu, I. Mann, J. Rae, J. Raeder, X. Li, W. Liu, H. J. Singer, V. A. Sergeev, S. Apatenkov, G. Parks, M. Fillingim, and J. Sigwarth, *Space Sci. Rev.* **141**(1–4), 453 (2008).
- ⁶F. S. Mozer, P. L. Pritchett, J. Bonnell, D. Sundkvist, and M. T. Chang, *J. Geophys. Res.* **113**, A00C03, doi:10.1029/2008JA013535 (2008).
- ⁷C. Torrence and G. P. Compo, *Bull. Am. Meteorol. Soc.* **79**, 61 (1998).
- ⁸F. S. Mozer and P. L. Pritchett, *Geophys. Res. Lett.* **36**, L07102, doi:10.1029/2009GL037463 (2009).
- ⁹S. D. Bale, F. S. Mozer, and T. Phan, *Geophys. Res. Lett.* **29**(24), 2180, doi:10.1103/PhysRevLett.89.015002 (2002).
- ¹⁰A. L. Verdon, I. H. Cairns, D. B. Melrose, and P. A. Robinson, *Phys. Plasmas* **16**, 052105 (2009).
- ¹¹P. Yoon, A. T. Y. Lui, and M. I. Sitnov, *Phys. Plasmas* **9**, 1526 (2002).
- ¹²W. Daughton, G. Lapenta, and P. Ricci, *Phys. Rev. Lett.* **93**, 105004 (2004).
- ¹³W. Daughton, *Phys. Plasmas* **10**, 3103 (2003).
- ¹⁴H. Ji, S. Terry, M. Yamada, R. Kulsrud, A. Kuritsyn, and Y. Ren, *Phys. Rev. Lett.* **92**, 115001 (2004).
- ¹⁵R. L. Stenzel, *Phys. Rev. Lett.* **38**(3), 394 (1977).